

Tune-out wavelengths for metastable helium

J. Mitroy¹ and Li-Yan Tang^{1,2}

¹*School of Engineering, Charles Darwin University, Darwin, Northern Territory 0909, Australia*

²*State Key Laboratory of Magnetic Resonance and Atomic and Molecular Physics, Wuhan Institute of Physics and Mathematics, Chinese Academy of Sciences, Wuhan 430071, People's Republic of China*

(Received 24 September 2013; published 20 November 2013)

The six longest tune-out wavelengths for the He($1s2s\ ^3S_1^e$) metastable state are determined by explicit calculation. The tune-out wavelength at 413.02 nm is expected to be sensitive to finite mass, relativistic, and quantum electrodynamic effects upon the transition matrix elements and its measurement would provide a nonenergy test of fundamental atomic structure theory.

DOI: [10.1103/PhysRevA.88.052515](https://doi.org/10.1103/PhysRevA.88.052515)

PACS number(s): 31.15.ap, 31.15.ac, 31.30.jc, 32.10.Dk

I. INTRODUCTION

The fundamental physics framework for high-precision calculations on light atomic systems is nonrelativistic quantum electrodynamics (NRQED) [1–3]. This approach starts with the nonrelativistic Hamiltonian and relativistic and quantum electrodynamic corrections are added by using perturbation theory [4–6]. Atomic structure calculations for systems with two or three electrons are often done with correlated basis sets and very high precision in calculations of energies have been achieved [3,7–9]. Energy corrections for finite nuclear mass and the finite nuclear volume can be included [7,10–12].

Many atomic properties are known to much lower degrees of precision than the energy. For example, calculations of rates for forbidden transitions require relativistic effects to be taken into consideration. However, the precision of experiments on such systems is not high. For example, the rate for the He($1s2p\ ^3P_1^o \rightarrow 1s^2\ ^1S_0^e$) transition has been measured to an accuracy of 4.5% [13]. This is typical of atomic physics, there are relatively few experimental determinations of atomic transition rates that have a precision of 0.1% or better [14].

At the present time, the most precise calculation of an atomic property that is dominated by atomic transition rate properties is the helium atom ground-state polarizability [15,16]. There is an experimental determination of this polarizability that is accurate to 9.1 ppm [17].

In this paper, we identify an atomic property that could be measured and provide a new test of NRQED. This property is the tune-out wavelength of the He($1s2s\ ^3S_1^e$) state. When an atom is immersed in an electric field it experiences an energy shift which is proportional to the square of the electric field. The electric field can be a static field or the field of an electromagnetic wave and the energy shift can be written [18,19] as

$$\Delta E \approx -\frac{1}{2}\alpha_d(\omega)F^2, \quad (1)$$

where $\alpha_d(\omega)$ is the dipole polarizability of the quantum state at frequency ω and F is the strength of the electromagnetic field. The value of the dynamic polarizability in the $\omega \rightarrow 0$ limit is the static dipole polarizability. The tune-out wavelength is the wavelength at which the polarizability goes to zero [20–22].

One method to determine the tune-out wavelength is to use an atom interferometer [23,24]. A beam of metastable helium would be split into two, with a laser irradiating one of the paths. The wavelength for which the phase shift is zero is the tune-

out wavelength. Since the measurement is a null experiment, the intensity and beam profile of the irradiating laser does not need to be known precisely. A tune-out wavelength has recently been measured to an accuracy of 2 ppm for potassium and has yielded a precise estimate of the oscillator strength ratio for the $4s \rightarrow 4p$ spin-orbit doublet [22,24]. Some tune-out wavelengths for rubidium have also been determined by the diffraction of a Bose-Einstein condensate off a series of standing wave pulses [25].

The present manuscript describes calculations of a number of tune-out wavelengths for the He($1s2s\ ^3S_1^e$) state. The purpose of the present paper is not to absolutely determine to maximum precision the specific values of the tune-out wavelengths. Rather, it is to give estimates of these wavelengths to an accuracy of about 0.2% to constrain the possible wavelength and thereby provide guidance to any experimental effort.

II. STRUCTURE MODEL

The He($1s2s\ ^3S_1^e$) state transition arrays were taken from two sources. Line strengths from Hylleraas calculations [26,27] were used for the transitions to the He($1s2p\ ^1,^3P_1^o$) and He($1s3p\ ^1,^3P_1^o$) states. They were extracted from tabulations of oscillator strengths and energy differences. These matrix elements were calculated including relativistic effects but did not include finite mass effects. The contributions from these manifolds of states make up 98% of the He($1s2s\ ^3S_1^e$) state polarizability.

The remainder of the polarizability was computed from a one-electron model of the structure of the helium triplet states. The frozen core model, consisted of a valence electron moving in the field of the He⁺($1s$) ground state. The direct and exchange interactions between the valence and core electrons were computed without approximation. A semiempirical core polarization potential, with the polarizability set to that of the He⁺($1s$) ground state, namely, $0.28125\ a_0^3$, was then tuned to reproduce the binding energies of the lowest state of each symmetry. The model Hamiltonian for the valence electron was then diagonalized in a large basis of Laguerre type orbitals (LTOs). The transition matrix elements between the ground and dipole excited states were computed with a modified transition operator [28,29]. This core-polarization model (CPM) of the helium structure is expected to be reliable. Similar models have been applied to describe the structures of many atoms with one or two valence electrons [28,30] and

TABLE I. Line strengths for some low-lying He transitions.

Transition	CPM	Hylleraas [26,27]
$1s2s\ ^3S_1^e \rightarrow 1s2p\ ^3P_0^o$	6.4175	6.404 439
$1s2s\ ^3S_1^e \rightarrow 1s2p\ ^3P_1^o$	19.253	19.215 27
$1s2s\ ^3S_1^e \rightarrow 1s2p\ ^3P_2^o$	32.0877	32.025 35
$1s2s\ ^3S_1^e \rightarrow 1s2p\ ^1P_1^o$		1.4878×10^{-6}
$1s2s\ ^3S_1^e \rightarrow 1s3p\ ^3P_0^o$	0.2729	0.274 990
$1s2s\ ^3S_1^e \rightarrow 1s3p\ ^3P_1^o$	0.8188	0.825 131
$1s2s\ ^3S_1^e \rightarrow 1s3p\ ^3P_2^o$	1.3646	1.374 964
$1s2s\ ^3S_1^e \rightarrow 1s3p\ ^1P_1^o$		1.4684×10^{-8}

give polarizabilities for atoms and ions lighter than sodium and magnesium that are accurate to better than 0.5% [19,30]. The differences between the CPM and experimental energies did not exceed 5×10^{-5} hartree, which suggests that the underlying model Hamiltonian is a reasonable model of the helium excitation spectrum.

Table I lists line strengths, S_{ij} , for some transitions where

$$S_{ij} = |\langle \psi_i; L_i J_i || r^k C^k(\hat{\mathbf{r}}) || \psi_j; L_j J_j \rangle|^2. \quad (2)$$

The CPM line strengths were computed in an L coupling scheme and transformed to an LSJ coupling scheme using standard expressions [31]. The better than 1% agreement between the CPM and Hylleraas line strengths suggests that the error introduced by using the CPM line strengths for the higher discrete and continuum excitations will be small.

The Hylleraas line strengths for the transitions to the $J = 0, 1$, and 2 states are very close to the 1 : 3 : 5 ratio that would be expected from purely geometric considerations. The deviation from this ratio is only 0.01% for the $\text{He}(1s2s\ ^3S_1^e \rightarrow 1s2p\ ^3P_J^o)$ multiplet and is even smaller for the $\text{He}(1s2s\ ^3S_1^e \rightarrow 1s3p\ ^3P_J^o)$ multiplet.

III. POLARIZABILITIES

A. Static polarizabilities

The $\text{He}(1s2s\ ^3S_1^e)$ polarizability is computed using the sum rule

$$\alpha_d(\omega) = \sum_i \frac{f_{ni}^{(1)}}{\Delta E_{ni}^2 - \omega^2}, \quad (3)$$

where $f_{ni}^{(1)}$ and ΔE_{ni} are the oscillator strength and excitation energy of a given transition and ω is the photon energy. Polarizabilities are computed using experimental energy differences [32] for the lowest-energy excited states. The contribution of the core is included in the CPM line-strength distribution [30] by using a pseudo-oscillator strength distribution constructed by diagonalizing the He^+ Hamiltonian in a basis of three $\ell = 1$ LTOs.

The present calculation, incorporating Hylleraas matrix elements for the transition to the $\text{He}(1s2p\ ^{1,3}P_J^o)$ and $\text{He}(1s3p\ ^{1,3}P_J^o)$ states and CPM matrix elements for the remaining transitions is termed the hybrid calculation. Hybrid calculations using matrix elements from different sources have been widely used for polarizability calculations [19,33,34].

Static polarizabilities for the $\text{He}(1s2s\ ^3S_1^e)$ state from a variety of source are listed in Table II. The hybrid calculation

TABLE II. Static dipole polarizabilities for the $\text{He}(1s2s\ ^3S_1^e)$ state.

	Year	α_d (a.u.)
Present: CPM	2013	316.020
Present: Hybrid	2013	315.462
Hylleraas [35]	1972	315.608
CI B spline [36]	1995	315.63
Hylleraas [37]	1998	315.631 468(12)
Experiment [38]	1977	301(20)
Experiment [39,40]	1995	322(6.8)

gives a dipole polarizability of $315.462 a_0^3$ for the $\text{He}(1s2s\ ^3S_1^e)$ state. This is about 0.05% smaller than the listed Hylleraas calculations, which give $315.63 a_0^3$ for the polarizability. Exact agreement with the Hylleraas calculations is not expected since these calculations are infinite mass calculations which do not include relativistic effects. About 96.5% of the polarizability comes from the transitions to the $\text{He}(1s2p\ ^3P_J^o)$ multiplet. The CPM calculation gave a polarizability of $316.020 a_0^3$, which is about 0.13% larger than that given by the Hylleraas calculations.

B. Dynamic polarizabilities and tune-out wavelengths

Figure 1 depicts the dynamic polarizability of the $\text{He}(1s2s\ ^3S_1^e)$ state as a function of energy. For purposes of simplicity the structure model used to create this plot did not allow for spin-orbit splitting and the very weak intercombination transitions. In this diagram, there is no tune-out wavelength in the vicinity of the $\text{He}(1s2p\ ^3P^o)$ excitation. Tune-out wavelengths occur just before the excitation thresholds for the $\text{He}(1s3p\ ^3P^o)$ and $\text{He}(1s4p\ ^3P^o)$ states. The tune-out frequency that would allow the easiest experimental investigation is just below the $\text{He}(1s3p\ ^3P^o)$ state.

The narrow spin-orbit splitting of the $\text{He}(^3P_J^o)$ states leads to the creation of additional tune-out frequencies and there are a total of six tune-out wavelengths below 0.118 a.u. photon energy. These tune-out wavelengths, along with a breakdown of the polarizability contributions are given in Table III. The differences between the hybrid model and the CPM values give a reasonable estimate of the uncertainty in the calculations. The derivative of the polarizability with

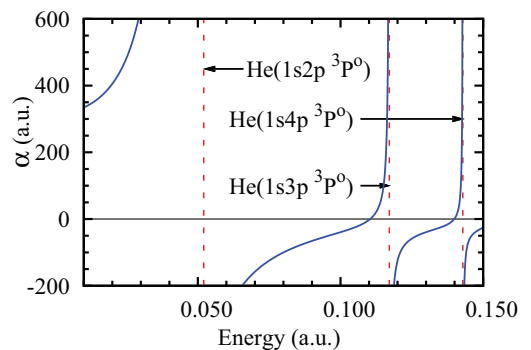


FIG. 1. (Color online) The dynamic polarizability of the $\text{He}(1s2s\ ^3S_1^e)$ state for photon energies below 0.150 a.u. This diagram does not include features due to spin-orbit splitting. Excitation thresholds are indicated as dashed lines.

TABLE III. Contributions to the polarizability at the tune-out wavelengths by using the hybrid line-strength set. The remainder term includes the core and all valence transitions other than those specifically listed.

λ_{to} (nm)	∞	1083.325 058	1083.219 229	886.609 509 91	413.019 405 0	388.974 876 3	388.971 133 2
ω_{to} (a.u.)	0	0.042 058 800 52	0.0 42 062 909 61	0.051 390 552 457	0.110 317 704 2	0.117 137 006 3	0.117 138 133 5
$\frac{d\alpha}{d\lambda}$ (a_0^3/nm)		-7.62×10^9	-1.13×10^8	-1.28×10^8	-1.913	-3.12×10^{10}	-1.00×10^9
CPM: λ_{to} (nm)	∞	1083.325 058	1083.219 230	886.609 510	412.801 707	388.974 876	388.971 133
$1s2p \ ^3P_2^o$	169.210	-1.6408×10^7	-8.2252×10^5	-343.232	-28.778	-25.043	-25.043
$1s2p \ ^3P_1^o$	101.526	1.6254×10^7	-5.3672×10^5	-205.948	-17.267	-15.026	-15.026
$1s2p \ ^3P_0^o$	33.835	1.5362×10^5	1.3592×10^6	-68.680	-5.756	-5.009	-5.009
$1s2p \ ^1P_1^o$	6.43×10^{-6}	1.95×10^{-5}	1.95×10^{-5}	605.341	-1.78×10^{-6}	-1.53×10^{-6}	-1.53×10^{-6}
$1s3p \ ^3P_2^o$	2.609	2.995	2.995	3.230	3.075	-2.4504×10^6	-1.2843×10^5
$1s3p \ ^3P_1^o$	1.565	1.797	1.797	1.939	13.847	2.4264×10^6	-8.4154×10^4
$1s3p \ ^3P_0^o$	0.522	0.599	0.599	0.646	4.614	2.4041×10^4	2.1261×10^5
Remainder	6.196	6.524	6.525	6.704	10.264	11.506	11.506
Total	315.462	0	0	0	0	0	0

wavelength is also tabulated. Only one of the wavelengths, that at 413.02 nm, can be classed as a useful probe of atomic structure. The tune-out wavelength triggered by the weak $\text{He}(1s2s \ ^3S_1^e \rightarrow 1s2p \ ^1P_1^o)$ transition is 4.6×10^{-6} nm away from the excitation wavelength and is barely detectable.

The dynamic polarizability in the vicinity of the $\text{He}(1s2p \ ^3P_J^o)$ excitations is depicted in Fig. 2. The additional tune-out frequencies lie between the $J = 0, 1$ and the $J = 1, 2$ states. The positions of the tune-out wavelengths here are largely determined by the energies of the $\text{He}(1s2p \ ^3P_J^o)$ states and the relative sizes of the line strengths to the $\text{He}(1s2p \ ^3P_J^o)$ states. The tune-out wavelengths caused by the spin-orbit transitions of the $\text{He}(1s2p \ ^3P_J^o)$ multiplet are at infrared wavelengths. The one between the $J = 0$ and $J = 1$ excitations at 1083.219 nm should be the easiest to detect due to the larger splitting of 0.159 nm between the two states. The experimental determination of this particular tune-out wavelength would mainly be of interest for diagnostic purposes. The dominant polarizability contributions come from the transitions to the states of the $\text{He}(1s2p \ ^3P_J^o)$ multiplet which are larger by a factor of 10^5 than the contributions from any other states. As mentioned earlier, the line strengths to the spin-orbit state are very close to a 1:3:5 ratio. Table III also lists the tune-out wavelengths from the CPM model which have line strengths exactly in the 1:3:5 ratio. The differences between the hybrid and CPM tune-out wavelengths

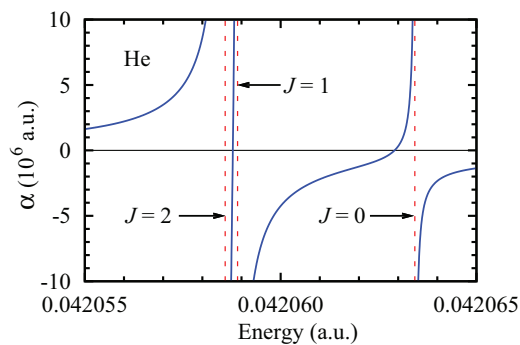


FIG. 2. (Color online) The dynamic polarizability of the $\text{He}(1s2s \ ^3S_1^e)$ state near the $\text{He}(1s2p \ ^3P_J^o)$ multiplet. The excitation thresholds for the spin-orbit states are indicated.

are negligible due to the close adherence of the hybrid lines strengths to the 1:3:5 ratio.

The $\text{He}(1s3p \ ^3P_J^o)$ multiplet results in three tune-out wavelengths. Two of these tune-out wavelengths occur in the energy intervals between the spin-orbit states. They occur at 388.9749 and 388.9711 nm. From Table III it is clear that the exact positions of the tune-out wavelengths will be dominated by the positive and negative contributions from the different transitions of the $\text{He}(1s3p \ ^3P_J^o)$ multiplet. Consequently, the position of the tune-out wavelengths will be determined by the 1:3:5 ratio of the three transitions to this multiplet. So these two tune-out wavelengths should be regarded as not interesting.

The tune-out wavelength that is most sensitive to true dynamical effects is at 413.02 nm. There are negative contributions to the polarizability from the $\text{He}(1s2p \ ^3P_J^o)$ multiplet while positive contributions come from the transitions to the $\text{He}(1s3p \ ^3P_J^o)$ multiplet and higher excitations. This tune-out wavelength can be used to test the accuracy of theoretical descriptions of the $\text{He}(1s2s \ ^3S_1^e)$ state. The dynamic polarizability near the tune-out wavelength can be described with a simple dynamical model where the polarizability due to the three transitions to the $\text{He}(1s3p \ ^3P_J^o)$ multiplet becomes large enough to cancel the negative polarizability arising from the $\text{He}(1s2s \ ^3S_1^e \rightarrow 1s2p \ ^3P_J^o)$ transitions. The tune-out wavelength is 24 nm longer than the excitation wavelengths of the states of the $\text{He}(1s3p \ ^3P_J^o)$ multiplet.

The variation of the polarizability with frequency in the vicinity of the 413.02-nm tune-out wavelength can be described by a simple two-component model previously applied to the alkaline-earth atoms [41]. One writes,

$$\alpha(\omega) = \alpha_0(\omega) + \frac{f}{\Delta E^2 - \omega^2}, \quad (4)$$

where α_0 is the background polarizability arising from all transitions except the transition near the tune-out wavelength, ΔE is the transition energy to the $\text{He}(1s3p \ ^3P_J^o)$ multiplet, and f is the oscillator strength to that multiplet. The variation of the background polarizability with frequency will be much slower than the variation of polarizability arising from the $\text{He}(1s2s \ ^3S_1^e \rightarrow 1s3p \ ^3P_J^o)$ transition. Making the simplification that α_0 is constant results in the following expression for the tune-out

frequency when $f/\alpha_0 \ll \Delta E$ [41],

$$\omega_{\text{to}} \approx \Delta E(1 + X_{\text{shift}}). \quad (5)$$

The quotient,

$$X_{\text{shift}} = f/(2\alpha_0 \Delta E^2), \quad (6)$$

is a relative energy shift and provides an estimate of the relative difference between the transition frequency and the tune-out frequency.

Equations (5) and (6) can be used for an uncertainty analysis. The tune-out frequency uncertainty is given by

$$\delta\omega_{\text{to}} = \Delta E \delta X_{\text{shift}}, \quad (7)$$

where

$$\frac{\delta X_{\text{shift}}}{X_{\text{shift}}} = \frac{\delta f}{f} + \frac{\delta\alpha_0}{\alpha_0}, \quad (8)$$

giving

$$\delta\omega_{\text{to}} = \Delta E X_{\text{shift}} \left(\frac{\delta f}{f} + \frac{\delta\alpha_0}{\alpha_0} \right). \quad (9)$$

The contribution to the uncertainty in X_{shift} due to the uncertainty in the transition energy does not have to be considered at the present level of accuracy. The terms on the right-hand side of Eq. (9) contain atomic structure information related to the transition moments for transitions originating from the $1s2s\ ^3S_1^e$ state. Suppose we write Y as a variable representing an atomic structure parameter and we replace the term in parentheses in Eq. (9) by $2\delta Y/Y$, we then obtain

$$\frac{\delta Y}{Y} = \frac{\delta\omega_{\text{to}}}{2\Delta E X_{\text{shift}}} \approx \left(\frac{\delta\lambda_{\text{to}}}{\lambda_{\text{to}}} \right) \frac{1}{2X_{\text{shift}}}. \quad (10)$$

This relation defines the precision with which structure information can be extracted from a measurement of the tune-out frequency. For the 413.02-nm tune-out wavelength, one has $X_{\text{shift}} = 0.0582$ and consequently $\frac{\delta Y}{Y} = 8.6(\delta\lambda_{\text{to}}/\lambda_{\text{to}})$.

Suppose the tune-out frequency can be determined to an absolute accuracy of 0.0001 nm, then the fractional uncertainty in the derived structure information would be 1.8×10^{-6} . This would constitute the most precise measurement of transition rate information ever made for helium. At the present time, the polarizability of the helium ground state has been measured to 9.1 ppm [17]. Finite mass effects in the form of a reduced mass effect and a mass polarization term make contributions to the helium ground-state polarizability of 137 and 35 ppm, respectively [15]. Relativistic effects of order α^2 and QED effects of order α^3 make a contribution at the level of 58 and 22 ppm, respectively [16,42]. A measurement of the 413.02-nm tune-out wavelength at an accuracy of 0.0001 nm would have the potential to probe QED effects in an atomic structure model of the helium metastable state.

There is one other polarizability parameter that relates to the feasibility of a tune-out measurement. It is the rate of change of the polarizability with wavelength. For the 413.02-nm tune-out wavelength, one has

$$\frac{d\alpha}{d\lambda} = -1.913 a_0^3/\text{nm}. \quad (11)$$

Table III gives this derivative for other tune-out wavelengths. This information provides a first indication of the strength of

the laser field and the offset from the tune-out wavelength necessary to create a detectable perturbation in the polarizability.

C. Uncertainty in the estimate of the tune-out wavelengths

In this section we estimate the uncertainty in the position of the 413.02-nm tune-out wavelength. The positions of the other five tune-out wavelengths are largely determined by the relative sizes of the transitions to the different states of the same multiplet. A conservative estimate of the uncertainties in these five tune-out wavelengths would be 10^{-6} nm or smaller, i.e., the difference between the hybrid and CPM estimates of λ_{to} .

Equation (8) is the basis for 413.02-nm tune-out wavelength uncertainty analysis. There are two quantities that largely determine the precise value of X_{shift} ; these are the $\text{He}(1s2s\ ^3S_1^e \rightarrow 1s3p\ ^3P^o)$ oscillator strength and the dynamic polarizability computed with this transition omitted from the sum rule. Some uncertainties will be estimated by reference to the basic structure of the helium triplet states, i.e., as a single electron moving in the field of a core with a net charge of unity.

For the purpose of this analysis the $1s2s\ ^3S_1^e \rightarrow 1s3p\ ^3P_1^o$ transitions are treated as a single transition. The total spin-orbit splitting of the $1s3p$ multiplet is 1.3×10^{-6} a.u., which is much smaller than the energy difference between the tune-out energy and the $1s3p\ ^3P^o$ state energy of 0.0066 a.u. There are two sources of uncertainty for this transition, these are the impact of finite mass and relativistic effects. The two states are treated as single-electron states for the estimation of the finite mass effect. The correction to the line strength will be approximately $2m_e/m_{\text{He}} = 2.74 \times 10^{-4}$. A reasonable estimate of the relativistic effect can be made by comparing the relativistic and nonrelativistic matrix elements for the $2s \rightarrow 3p_J$ transitions for hydrogen. This ratio is 0.999 91 for the $2s \rightarrow 3p_{3/2}$ transition and 0.999 97 for the $2s \rightarrow 3p_{1/2}$ transition. The relativistic correction is taken to be 0.9×10^{-4} , i.e., the larger of the two corrections. So the relative uncertainty in the $1s2s\ ^3S_1^e \rightarrow 1s3p\ ^3P^o$ oscillator strength is set to 3.6×10^{-4} . This analysis does not include any calculational error due to the Hylleraas calculation since the purely calculational error would be much smaller than the other sources of uncertainties identified above.

The estimation of the uncertainty in the polarizability, $\alpha(\omega)$, is divided into two parts; the first is due to the contributions from the resonant $\text{He}(1s2s\ ^3S_1^e \rightarrow 1s2p\ ^3P_1^o)$ transitions and the second is due to the remainder term. First consider the $1s2s\ ^3S_1^e \rightarrow 1s2p\ ^3P_1^o$ transitions. Once again the finite mass correction will be approximately $2m_e/m_{\text{He}} = 2.74 \times 10^{-4}$. The relativistic effect in this case, once again deduced by comparison of nonrelativistic and Dirac equation line strengths, was 0.5×10^{-4} . The net uncertainty in that part of the polarizability due to this transition was 0.017 a.u.

The difference between the CPM and Hylleraas line strengths for the $\text{He}(1s2s\ ^3S_1^e \rightarrow 1s3p\ ^3P_1^o)$ transitions does not exceed 1.1%. This uncertainty is taken as typical of the line-strength uncertainties in the calculation of the remainder term, which consequently has an uncertainty of 0.11 a.u. This is about the same size as the known error in the polarizability in similar calculations for Li, namely, 0.10 a.u. or 0.06% [43,44]. So the assignment of an uncertainty of 0.11 a.u. for the remainder is reasonable given that a similar methodology

yields an error of 0.10 a.u. in the total dipole polarizability for the larger lithium atom. Substituting these uncertainty estimates into the relation

$$X_{\text{shift}} = \frac{f_{3p}}{2(\alpha_{2p} + \alpha_{\text{remainder}})\Delta E^2} \quad (12)$$

gives $\Delta X_{\text{shift}}/X_{\text{shift}} = 0.0035$. This translates into an overall uncertainty in the 413.02-nm tune-out wavelength of 0.09 nm. This is about half the size of the difference between the CPM and hybrid model estimates. The dominant contribution to the uncertainty comes from $\alpha_{\text{remainder}}$. There are other contributions to the uncertainty, but they would be much smaller than the already included uncertainties.

IV. CONCLUSION

The tune-out wavelengths for the $\text{He}(1s2s\ ^3S^e)$ state have been estimated from a hybrid structure model. The tune-out wavelength at 413.02 nm could conceivably be used to probe atomic structure models at a precision that is sensitive to finite mass, relativistic, and QED effects. A precision of 0.0001 nm in the measured tune-out wavelength would test structure information related to transition matrix elements to an overall

accuracy of 2 ppm. Such a measurement would open a new avenue to test fundamental atomic structure theory, at the present time there are no high-precision calculations for helium that incorporate both finite mass and relativistic effects in the transition matrix elements.

There is one other possible experiment involving cold metastable helium atoms that would also be sensitive to relativistic and QED effects. That would be to measure the magic wavelengths for the $\text{He}(1s2s\ ^3S^e \rightarrow 1s2p\ ^3P^o)$ transitions for a cloud of ultracold helium atoms. It would be worthwhile to determine the magic wavelengths that would be the best atomic structure probes.

ACKNOWLEDGMENTS

The work was supported by the Australian Research Council Discovery Project DP-1092620, the National Basic Research Program of China under Grant No. 2012CB821305, and the NNSF of China under Grants No. 11104323 and No. 11034009. The authors would like to thank Dr. Jun Jiang for performing calculations of the hydrogen atom matrix elements using the Dirac equation.

-
- [1] W. E. Caswell and G. P. Lepage, *Phys. Lett. B* **167**, 437 (1986).
 - [2] K. Pachucki, *Phys. Rev. A* **56**, 297 (1997).
 - [3] J. Mitroy, S. Bubin, W. Horiuchi, Y. Suzuki, L. Adamowicz, W. Cencek, K. Szalewicz, J. Komasa, D. Blume, and K. Varga, *Rev. Mod. Phys.* **85**, 693 (2013).
 - [4] K. Pachucki, *J. Phys. B* **35**, 3087 (2002).
 - [5] A. Yelkhovsky, *Phys. Rev. A* **64**, 062104 (2001).
 - [6] K. Pachucki, *Phys. Rev. A* **74**, 062510 (2006).
 - [7] G. W. F. Drake, W. Nortershauser, and Z. C. Yan, *Can. J. Phys.* **83**, 311 (2005).
 - [8] K. Pachucki and J. Komasa, *Phys. Rev. Lett.* **92**, 213001 (2004).
 - [9] M. Stanke, J. Komasa, D. Kędziera, S. Bubin, and L. Adamowicz, *Phys. Rev. A* **78**, 052507 (2008).
 - [10] Z.-C. Yan and G. W. F. Drake, *Phys. Rev. A* **66**, 042504 (2002).
 - [11] M. Stanke, D. Kędziera, S. Bubin, and L. Adamowicz, *Phys. Rev. A* **77**, 022506 (2008).
 - [12] M. Puchalski and K. Pachucki, *Phys. Rev. A* **78**, 052511 (2008).
 - [13] R. G. Dall, K. G. H. Baldwin, L. J. Byron, and A. G. Truscott, *Phys. Rev. Lett.* **100**, 023001 (2008).
 - [14] N. Bouloufa, A. Crubellier, and O. Dulieu, *Phys. Scr., T* **T134**, 014014 (2009).
 - [15] W. Cencek, K. Szalewicz, and B. Jeziorski, *Phys. Rev. Lett.* **86**, 5675 (2001).
 - [16] G. Łach, B. Jeziorski, and K. Szalewicz, *Phys. Rev. Lett.* **92**, 233001 (2004).
 - [17] J. W. Schmidt, R. M. Gaviolo, E. F. May, and M. R. Moldover, *Phys. Rev. Lett.* **98**, 254504 (2007).
 - [18] T. M. Miller and B. Bederson, *Adv. At. Mol. Phys.* **13**, 1 (1977).
 - [19] J. Mitroy, M. S. Safronova, and C. W. Clark, *J. Phys. B* **43**, 202001 (2010).
 - [20] L. J. LeBlanc and J. H. Thywissen, *Phys. Rev. A* **75**, 053612 (2007).
 - [21] B. Arora, M. S. Safronova, and C. W. Clark, *Phys. Rev. A* **84**, 043401 (2011).
 - [22] J. Jiang, L. Y. Tang, and J. Mitroy, *Phys. Rev. A* **87**, 032518 (2013).
 - [23] A. D. Cronin, J. Schmiedmayer, and D. E. Pritchard, *Rev. Mod. Phys.* **81**, 1051 (2009).
 - [24] W. F. Holmgren, R. Trubko, I. Hromada, and A. D. Cronin, *Phys. Rev. Lett.* **109**, 243004 (2012).
 - [25] C. D. Herold, V. D. Vaidya, X. Li, S. L. Rolston, J. V. Porto, and M. S. Safronova, *Phys. Rev. Lett.* **109**, 243003 (2012).
 - [26] G. W. F. Drake and D. C. Morton, *Astrophys. J., Suppl. Ser.* **170**, 251 (2007).
 - [27] D. C. Morton and G. W. F. Drake, *Phys. Rev. A* **83**, 042503 (2011).
 - [28] J. Mitroy, D. C. Griffin, D. W. Norcross, and M. S. Pindzola, *Phys. Rev. A* **38**, 3339 (1988).
 - [29] S. Hameed, A. Herzenberg, and M. G. James, *J. Phys. B* **1**, 822 (1968).
 - [30] J. Mitroy and M. W. J. Bromley, *Phys. Rev. A* **68**, 052714 (2003).
 - [31] B. W. Shore and D. H. Menzel, *Principles of Atomic Spectra* (Wiley & Sons, New York, 1968).
 - [32] A. Kramida, Y. Ralchenko, J. Reader, and NIST ASD Team, NIST Atomic Spectra Database, Version 5.0.0, 2012, <http://physics.nist.gov/asd>.
 - [33] M. S. Safronova, W. R. Johnson, and A. Derevianko, *Phys. Rev. A* **60**, 4476 (1999).
 - [34] S. G. Porsev and A. Derevianko, *J. Exp. Theor. Phys.* **102**, 195 (2006).
 - [35] G. W. F. Drake, *Can. J. Phys.* **50**, 1896 (1972).
 - [36] M. K. Chen, *J. Phys. B* **28**, 1349 (1995).
 - [37] Z.-C. Yan and J. F. Babb, *Phys. Rev. A* **58**, 1247 (1998).
 - [38] D. A. Crosby and J. C. Zorn, *Phys. Rev. A* **16**, 488 (1977).

- [39] C. R. Ekstrom, J. Schmiedmayer, M. S. Chapman, T. D. Hammond, and D. E. Pritchard, *Phys. Rev. A* **51**, 3883 (1995).
- [40] R. W. Molof, H. L. Schwartz, T. M. Miller, and B. Bederson, *Phys. Rev. A* **10**, 1131 (1974).
- [41] Y. Cheng, J. Jiang, and J. Mitroy, *Phys. Rev. A* **88**, 022511 (2013).
- [42] K. Pachucki and J. Sapirstein, *Phys. Rev. A* **63**, 012504 (2000).
- [43] J. Y. Zhang, J. Mitroy, and M. W. J. Bromley, *Phys. Rev. A* **75**, 042509 (2007).
- [44] L. Y. Tang, M. W. J. Bromley, Z. C. Yan, and J. Mitroy, *Phys. Rev. A* **87**, 032507 (2013).